Non-localité et contextualité, ou théorèmes de Bell et Kochen-Specker, et dessins d'enfants

Michel Planat

Institut FEMTO-ST, CNRS, 32 Avenue de l'Observatoire, F-25044 Besançon
(michel.planat@femto-st.fr)

Séminaires μ Φ, 18 février 2014, Besançon

Abstract[1,2]

- En mécanique quantique, le **théorème de Bell** interdit l'existence des théories à variables cachées locales (voulues par Einstein) tandis que le **théorème de Kochen-Specker** interdit aussi les théories non contextuelles.
- En **première partie**, je présente une interprétation par les géométries finies de ces théorèmes, à l'aide du groupe de Pauli des observables à deux ou trois qubits. En **deuxième partie**, je montre que ces géométries se construisent naturellement grâce aux dessins d'enfants de Grothendieck.
- D'où il suit une remarquable adéquation entre les 'mystères' quantiques et mathématiques, via **le groupe de Galois absolu du corps** $\mathbb{Q}$. Je propose aussi une notion d'**information stockée dans les hyperplans**.

[1] M. Planat, On small proofs of the Bell-Kochen-Specker theorem for two, three and four qubits, *EPJ Plus* **127**, 86 (2012).

[2] M. Planat, A. Giorgetti, F. Holweck and M. Saniga, Quantum contextual finite geometries from *dessins d'enfants*, Preprint 1310.4267 [quant-ph].

In a theory in which parameters are added to quantum mechanics to determine the results of individual measurements, without changing the statistical predictions, there must be a mechanism whereby the setting of one measuring device can influence the reading of another instrument, however remote (Bell 1964).

- Suppose we have four observables σ_i, $i = 1, 2, 3, 4$, taking values in $\{-1, 1\}$, of which Bob can measure (σ_1, σ_3) and Alice (σ_2, σ_4). The **Bell-CHSH approach to quantum contextuality/non-locality** consists of defining the number

$$C = \sigma_2(\sigma_1 + \sigma_3) + \sigma_4(\sigma_3 - \sigma_1) = \pm 2$$

and observing the (so-called Bell-CHSH) inequality [3]

$$|\langle\sigma_1\sigma_2\rangle + \langle\sigma_2\sigma_3\rangle + \langle\sigma_3\sigma_4\rangle - \langle\sigma_4\sigma_1\rangle| \leq 2,$$

where $\langle\rangle$ here means that we are taking averages over many experiments.

[3] A. Peres, Quantum theory: concepts and methods (Kluwer, 1995).

The square geometry of Bell's theorem: 2

- This inequality holds for any dichotomic random variables σ_i. **Bell's theorem** states that the inequality is violated if one considers **quantum observables with dichotomic eigenvalues**. An example is

$$\sigma_1 = I \otimes X,\ \sigma_2 = X \otimes I,\ \sigma_3 = I \otimes Z,\ \sigma_4 = Z \otimes I$$

$$C^2 = 4 * I + [\sigma_1, \sigma_3][\sigma_2, \sigma_4] = 4 \begin{pmatrix} 1 & . & . & 1 \\ . & 1 & \bar{1} & . \\ . & \bar{1} & 1 & . \\ 1 & . & . & 1 \end{pmatrix}$$

has eigenvalues 0 and 8, both with multiplicity 2 ($\bar{1} \equiv -1$). Using the norm $||A|| = sup(||A\psi||/||\psi||), \psi \in \mathcal{H}$, one arrives at the **maximal violation of the Bell-CHSH inequality** $||C|| = 2\sqrt{2}$.

The point-line incidence geometry associated with our four observables is one of the simplest, that of a **square**. There are 90 distinct squares among two-qubit observables and 30240 when three-qubit labeling is employed, each yielding a maximal violation of the Bell-CHSH inequality.

Peres, 1995: *There is no escape from nonlocality. The experimental violation of Bell's inequality leaves only two possibilities:* **either** *some simple physical observers (such as correlated photon pairs) are essentially nonlocal,* **or** *it is forbidden to consider simultaneously the possible outcomes of mutually exclusive experiments, even though any one of these experiments is actually realizable. The second alternative effectively rules out the introduction of exophysical automatons with a random behavior-let alone observers endowed with free will. If you are willing to accept that option,* **then it is the entire universe which is an indivisible, nonlocal entity.**

The Bell-Kochen-Specker theorem: 1

- The **Bell-Kochen-Specker proof** demonstrates the impossibility of Einstein's assumption, made in the famous Einstein-Podolsky-Rosen paper [4], that quantum mechanical observables represent 'elements of physical reality'. More specifically, the theorem **excludes hidden variable theories** that require elements of physical reality to be **non-contextual** (i.e. independent of the measurement arrangement) [5]
- **Essence of the BKS proof**: even for compatible observables A and B with values $v(A)$ and $v(B)$, the equations $v(aA + bB) = av(A) + bv(B)$ $(a, b \in \mathbb{R})$ or $v(AB) = v(A)v(B)$ may be violated.

[4] A. Einstein, B. Podolsky and N. Rosen, "Can quantum-mechanical description of physical reality be considered complete?" Phys. Rev. 47, 77780 (1935).

[5] Kochen S. and Specker E. P. 1967 The problem of hidden variables in quantum mechanics *J. Math. Mech.* **17** 59–87.

The Bell-Kochen-Specker theorem: 2

- A **non-coloring BKS proof** consists of a finite set of rays/vectors that cannot be assigned truth values (1 for true, 0 for false) in such a way that (i) one member of each complete orthonormal basis is true and (ii) no two orthogonal (that is, mutually compatible) projectors are both true.
  The smallest state-independent proofs in three dimensions are of the $31-17$ type (31 rays located on 17 orthogonal triads)[6].
- A **parity proof of BKS theorem** is a set of v rays that form l bases (l odd) such that each ray occurs an even number of times over these bases. A proof of BKS theorem is **ray critical** (resp. **basis critical**) if it cannot be further simplified by deleting even a single ray (resp. a single basis).
  The **smallest BKS proof** in dimension 4 (resp. 8) is a parity proof and corresponds to arrangements of real states arising from the two-qubit (resp. three-qubit) **Pauli group**, more specifically as eigenstates of operators forming Mermin's square (resp. Mermin's pentagram) [7].

[6] Peres A. 1993 *Quantum theory: concepts and methods* (Kluwer.

[7] Cabello A., Estebaranz J. M. and García-Alcaine G. 1996 Bell-Kochen-Specker theorem: A proof with 18 vectors *Phys. Lett. A* **212** 183–187.

The distance between the maximal orthonormal bases

Apart from the use of standard graph theoretical tools for characterizing the ray/base symmetries, we shall employ a useful signature of the proofs in terms of **Bengtsson's distance** D_{ab} between two orthonormal bases a and b defined as [8]

$$D^2_{ab} = 1 - \frac{1}{d-1} \sum_{i,j}^{d} \left(|\langle a_i | b_j \rangle|^2 - \frac{1}{d} \right)^2 . \quad (1)$$

The distance (1) vanishes when the bases are the same and is maximal (equal to unity) when the two bases a and b are mutually unbiased, $|\langle a_i | b_j \rangle|^2 = 1/d$, and only then. We shall see that the bases of a BKS proof employ a selected set of distances which seems to be a universal feature of the proof.

[8] Raynal P., Lü X. and Englert B.-G. 2011 Mutually unbiased bases in six dimensions: the four most distant bases *Phys. Rev. A* **83** 062303.

The Peres-Mermin square: an operator parity proof of 2QB BKS theorem [9]

We denote by X, Z and Y the **Pauli spin matrices** in x, y and z directions, and the tensor product is not explicit, i. e. for two qubits one denotes $Z_1 = Z \otimes I$, $Z_2 = I \otimes Z$ and $ZZ = Z \otimes Z$, for three qubits one denotes $Z_1 = Z \otimes I \otimes I$ and so on.

$$\begin{array}{ccc} | & | & || \\ -Z_1- & Z_2- & ZZ-_{I} \\ | & | & || \\ -X_2- & X_1- & XX-_{I} \\ | & | & || \\ -ZX- & XZ- & YY-_{I} \\ |_{I} & |_{I} & ||_{-I} \end{array} \qquad (2)$$

There is no way of assigning multiplicative properties to the eigenvalues ± 1 of the nine operators while still keeping the same multiplicative properties for the operators.

[9] Mermin N. D. 1993 Hidden variables and the two theorems of John Bell *Rev. Mod. Phys.* **65** 803-815.

2QB real eigenvectors and their maximal orthonormal bases

- 6 (operator) bases $\times 4$ (eigenstates) $=$ 24 real eigenstates/rays

$$\begin{array}{c} 1:[1000],\ \ 2:[0100],\ \ 3:[0010],\ \ 4:[0001],\ \ 5:[1111],\ \ 6:[11\bar{1}\bar{1}] \\ 7:[1\bar{1}1\bar{1}],\ \ 8:[1\bar{1}\bar{1}1],\ \ 9:[1\bar{1}\bar{1}\bar{1}],\ \ 10:[1\bar{1}11],\ \ 11:[11\bar{1}1],\ \ 12:[111\bar{1}] \\ 13:[1100],\ \ 14:[1\bar{1}00],\ \ 15:[0011],\ \ 16:[001\bar{1}],\ \ 17:[0101],\ \ 18:[010\bar{1}] \\ 19;[1010],\ \ 20:[10\bar{1}0],\ \ 21:[100\bar{1}],\ \ 22:[1001],\ \ 23:[01\bar{1}0],\ \ 24:[0110] \end{array} \tag{3}$$

- 24 complete orthogonal bases (numbered in blue)

$$\begin{array}{c} 1\text{: }\{1,2,3,4\}, 2\text{: }\{5,6,7,8\}, 3\text{: }\{9,10,11,12\}, 4\text{: }\{13,14,15,16\}, \\ 5\text{: }\{17,18,19,20\}, 6\text{: }\{21,22,23,24\}, 7\text{: }\{1,2,15,16\}, 8\text{: }\{1,3,17,18\}, \\ 9\text{: }\{1,4,23,24\}, 10\text{: }\{2,3,21,22\}, 11\text{: }\{2,4,19,20\}, 12\text{: }\{3,4,13,14\}, \\ 13\text{: }\{5,6,14,16\}, 14\text{: }\{5,7,18,20\}, 15\text{: }\{5,8,21,23\}, 16\text{: }\{6,7,22,24\}, \\ 17\text{: }\{6,8,17,19\}, 18\text{: }\{7,8,13,15\}, 19\text{: }\{9,10,13,16\}, 20\text{: }\{9,11,18,19\}, \\ 21\text{: }\{9,12,22,23\}, 22\text{: }\{10,11,21,24\}, 23\text{: }\{10,12,17,20\}, 24\text{: }\{11,12,14,15\} \end{array} \tag{4}$$

The diagram for a $18-9$ proof

The diagram for the $18-9$ proof is simply a 3×3 square. **There are** 18 **(distinct) edges that encode the** 18 **rays**, a selected vertex/base of the graph is encoded by the union of the four edges/rays that are adjacent to it.

$$\begin{array}{ccc}
\begin{pmatrix} 1 & 2 \\ 15 & 16 \end{pmatrix} - 1 - & \begin{pmatrix} 1 & 3 \\ 17 & 18 \end{pmatrix} - 3 - & \begin{pmatrix} 2 & 3 \\ 21 & 22 \end{pmatrix} - 2 \\
|_{16} & |_{18} & |_{22} \\
\begin{pmatrix} 5 & 6 \\ 14 & 16 \end{pmatrix} - 5 - & \begin{pmatrix} 5 & 7 \\ 18 & 20 \end{pmatrix} - 7 - & \begin{pmatrix} 6 & 7 \\ 22 & 24 \end{pmatrix} - 6 \\
|_{14} & |_{20} & |_{24} \\
\begin{pmatrix} 11 & 12 \\ 14 & 15 \end{pmatrix} - 12 - & \begin{pmatrix} 10 & 12 \\ 17 & 20 \end{pmatrix} - 10 - & \begin{pmatrix} 10 & 11 \\ 21 & 24 \end{pmatrix} - 11 \\
|_{15} & |_{17} & |_{21}
\end{array} \quad (5)$$

As for the **distances** between the bases, two bases located in the same row (or the same column) have distance $a_2 = \sqrt{7/12}$, while two bases not in the same row (or column) have distance $a_4 = \sqrt{5/6} > a_2$.

the **five distances** involved

$$D = \{a_1, a_2, a_3, a_4, a_5\} = \{\frac{1}{\sqrt{3}}, \frac{\sqrt{7}}{\sqrt{12}}, \frac{\sqrt{2}}{\sqrt{3}}, \frac{\sqrt{5}}{\sqrt{6}}, 1\}.$$

proof $v - l$	# proofs	a_1	a_2	a_3	a_4	a_5
$24 - 15$	16	18	18	9	54	6
$22 - 13A$	96	12	18	3	42	3
$22 - 13B$	144	12	18	4	42	2
$20 - 11A$	96	6	18	0	30	1
$20 - 11B$	144	6	18	1	30	0
$18 - 9$	16	0	18	0	18	0

- The histogram of distances. The symmetry group of Mermin's graph is $G_{72} = \mathbb{Z}_3^2 \rtimes D_4$. It governs most of the above 2^9 proofs although there also exist some extra abelian symmetries. Another nice geometrical display of the proofs is in *Waegell M. and Aravind P. K. 2011 Parity proofs of the Kochen-Specker theorem based on the* 24 *rays of Peres Found. Phys.* **41** *1786-1799.*).

The Mermin'spentagram (in square form): an operator parity proof of 3QB BKS theorem [10]

As for the 2QB Mermin's square, there is no way of assigning multiplicative properties to the eigenvalues ± 1 of the nine operators while still keeping the same multiplicative properties for the operators.

$$\begin{array}{ccccccccc} & | & & | & & | & & | & \\ & Z_1 & & Z_1 & & X_1 & & X_1 & \\ & | & & | & & | & & | & \\ & Z_2 & & X_2 & & Z_2 & & X_2 & \\ & | & & | & & | & & | & \\ & Z_3 & & X_3 & & X_3 & & Z_3 & \\ & | & & | & & | & & | & \\ = & ZZZ & = & ZXX & = & XZX & = & XXZ & = {\color{red}-I} \\ & |{\color{red}I} & & |{\color{red}I} & & |{\color{red}I} & & |{\color{red}I} & \end{array} \qquad (6)$$

In *Saniga M. and Lévay P. 2012 Mermin's pentagram as an ovoid of* $PG(3,2)$ *EPL* **97** *50006.* , it is shown that Mermin's pentagram corresponds to an ovoid of the three-dimensional projective space of order two, $PG(3,2)$.

[10] Mermin N. D. 1993 Hidden variables and the two theorems of John Bell *Rev. Mod. Phys.* **65** 803-815.

3QB real eigenvectors and their maximal orthonormal bases

$$
\begin{gathered}
1:[10000000],2:[01000000],3:[00100000],4:[00010000],5:[00001000],\\
6:[00000100],7:[00000010],8:[00000001],9:[11110000],10:[11\bar{1}\bar{1}0000],\\
11:[1\bar{1}1\bar{1}0000],12:[1\bar{1}\bar{1}10000],13:[00001111],14:[000011\bar{1}\bar{1}],15:[00001\bar{1}1\bar{1}],\\
16:[00001\bar{1}\bar{1}1],17:[11001100],18:[1100\bar{1}\bar{1}00],19:[1\bar{1}001\bar{1}00],20:[1\bar{1}00\bar{1}100],\\
21:[00110011],22:[001100\bar{1}\bar{1}],23:[001\bar{1}001\bar{1}],24:[001\bar{1}00\bar{1}1],25:[10101010],\\
26:[1010\bar{1}0\bar{1}0],27:[10\bar{1}010\bar{1}0],28:[10\bar{1}0\bar{1}010],29:[01010101],30:[01010\bar{1}0\bar{1}],\\
31:[010\bar{1}010\bar{1}],32:[010\bar{1}0\bar{1}01],33:[100101\bar{1}0],34:[100\bar{1}0110],35:[10010\bar{1}10],\\
36:[100\bar{1}0\bar{1}\bar{1}0],37:[0110\bar{1}001],38:[01\bar{1}01001],39:[01\bar{1}0\bar{1}00\bar{1}],40:[0110100\bar{1}].
\end{gathered}
\tag{7}
$$

The $5 \times 8 = 40$ real rays form 25 maximal orthogonal bases.

Distance signature of the 3QB proofs

$$D = \{a_1, a_2, a_3\} = \{\frac{\sqrt{3}}{\sqrt{7}}, \frac{\sqrt{9}}{\sqrt{14}}, \frac{\sqrt{6}}{\sqrt{7}}\}$$

proof $v - l$	# proofs	a_1	a_2	a_3
40 – 15	64	20	30	55
38 – 13	640	12	30	26
36 – 11	320	4	30	21

- The histogram of distances for the 2^{10} 3QB BKS proofs.

A schematic diagram for a $36-11$ proof

- Let us look at a $36-11$ parity proof. The 11 bases are displayed as a **pentagram** plus the isolated base 1.

$$\begin{array}{ccccccccccc} & & & & 2 & & & & & & \\ 6 & - & & 7 & - & 8 & & - & 9 & == & 1 \\ & & 10 & & & & 11 & & & & \\ & & & & 3 & & & & & & \\ & 4 & & & & & & 5 & & & \end{array} \tag{8}$$

- Two adjacent bases of the pentagram have **two rays** in common. The reference base has with each of the bases on the horizontal line of the pentagram **four rays** in common and is disjoint from any other base. Each line of the pentagram shares a set of four rays that is **disjoint** from the set of four rays shared by another line. The automorphism group of this configuration is isomorphic to S_5.
- The maximal distance, a_3, is that between two disjoint bases, and amounts to $\sqrt{6/7}$. The intermediate distance, $a_2 = \sqrt{9/14}$, occurs between two bases located in any line of the pentagram. Finally, the shortest distance, $a_1 = \sqrt{3/7}$, is that between the reference base and each of the four bases on the horizontal line of the pentagram. Similar diagrams can be produced for any proof.

Groth. 1: the absolute Galois group[11]

Whereas in my research before 1970, my attention was systematically directed towards objects of maximal generality, in order to uncover a general language adequate for the world of algebraic geometry, and I never restricted myself to algebraic curves except when strictly necessary (notably in etale cohomology), preferring to develop pass-key techniques and statements valid in all dimensions and in every place (I mean, over all base schemes, or even base ringed topoi...), here I was brought back, **via objects so simple that a child learns them while playing, to the beginnings and origins of algebraic geometry**, *familiar to Riemann and his followers!*

- Grothendieck's *dessins d'enfants* are (but are not just) bipartite graphs drawn on a smooth surface. They are the backdoor of the rich and still not fully explored world of algebraic numbers $\bar{\mathbb{Q}}$ and its group of symmetries, the so-called absolute Galois group $\mathrm{Gal}(\bar{\mathbb{Q}}/\mathbb{Q})$.

[11] A. Grothendieck, Sketch of a programme, written in 1984 and reprinted with translation in L. Schneps and P. Lochak (eds.), Geometric Galois Actions: 1. Around Grothendieck's Esquisse d'un Programme, and 2. The inverse Galois problem, Moduli Spaces and Mapping Class Groups (Cambridge Press, 1997).

Recovering an octahedron: index 6 in C_2^+

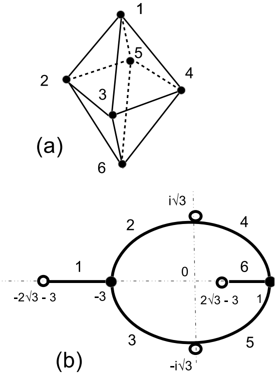

- A *dessin* (b) for the octahedron shown in (a). $P = \langle \alpha, \beta \rangle = \langle (1,2,3)(4,5,6),(2,4)(3,5) \rangle \cong A_4$; $s = (2,4,2,0)$; cycles:=$[3^2, 2^2 1^2, 3^2]$. Belyi function $f(x) = -\frac{1}{64x^3}(x-1)^3(x+3)^3$.

Recovering a generalized hexagon: index 63 in C_2^+

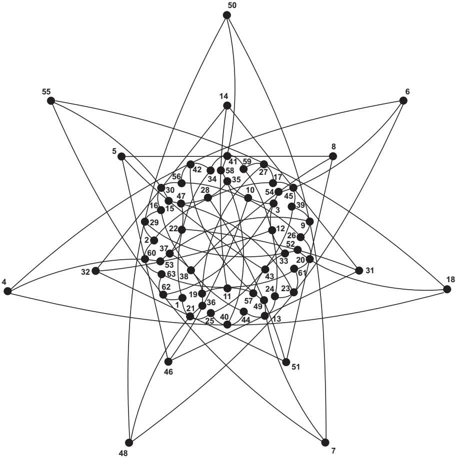

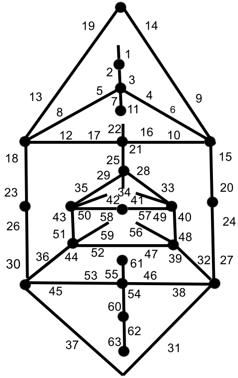

- A *dessin* (right) for the generalized hexagon $GH(2,2)$ (left).

Groth. 2: permutation group, signature and passport

- A dessin d'enfant is a pair $(X,\mathcal{D})$ made of an oriented compact topological surface X and a finite connected bicoloured graph $\mathcal{D}$ drawn on it. The vertices are given the colours **black** or **white**, an edge is given two different colours and the set difference $X \setminus \mathcal{D}$ is the union of finitely many topological discs, that are called the faces of $\mathcal{D}$ [12].
- To a dessin $\mathcal{D}$ with n edges $[1..n]$ one associate a permutation group $P = \langle \alpha, \beta \rangle$ on the set of labels such that a cycle of α (resp. β) contains the labels of the edges incident to a black vertex (resp. white vertex).
- The **Euler characteristic** of $\mathcal{D}$ is defined as $2 - 2g = B + W + F - n$, where B, W and n stands for the number of black vertices, the number of white vertices and the number of edges, respectively. A *dessin* $\mathcal{D}$ is ascribed a **signature** $s = (B, W, F, g)$ and a **passport** in the form $[C_\alpha, C_\beta, C_\gamma]$, where the entry C_i, $i \in \{\alpha, \beta, \gamma\}$ has factors $l_i^{n_i}$, with l_i denoting the length of the cycle and n_i the number of cycles of length l_i.

[12] S. K. Lando and A. K. Zvonkin, Graphs on surfaces and their applications (Springer Verlag, 2004).

Groth. 3: The cartographic group

- We restict to $\mathcal{D}$'s of the so-called **pre-clean type** that have the valency of white vertices ≤ 2.
  Dessins are in **one-to-one correspondence with conjugacy classes of subgroups** of finite index of the triangle group (cartographic group)

$$C_2^+ = \left\langle \rho_0, \rho_1, \rho_2 | \rho_1^2 = \rho_0\rho_1\rho_2 = 1 \right\rangle .$$

- The number of such *dessins* grows quite rapidly

$$1, 3, 3, 10, 15, 56, 131, 482, 1551, 5916, 22171, 90033, 370199, \cdots$$

.

- One proceeds by coset enumeration, that is, one counts the cosets of a subgroup H of C_2^+ and determines the corresponding permutation representation P (Todd-Coxeter algorithm) (with Magma [13]).

[13] $deg := n; F < x, y >:= FreeGroup(2); G < a, b >:= quo < F|y^2 >; low := LowIndexSubgroups(G, deg); Set := []; for\ \ k\ \ in\ \ [1..\#low]\ \ do\ \ H := low[k]; V := CosetSpace(G, H); f, P := CosetAction(V); if\ \ IsIsomorphic(P, SmallGroup(72, 40))\ \ eq\ \ true\ \ then\ \ k; Set := Append(Set, k);\ \ end\ \ if;\ \ end\ \ for;\ \ Set;$

Groth. 4: Belyi's theorem

- Belyi's theorem: a dessin may also been seen as a compact Riemann surface $\mathcal{S}$ defined over the field $\bar{\mathbb{Q}}$ of algebraic numbers. The Belyi function is $f : \mathcal{S} \to \mathbb{P}^1$, where $\mathbb{P}^1$ is the Riemann sphere with at most three branching values.
- Technically, given $f(x)$, a rational function of the complex variable x, a **critical point** of f is a root of its derivative and a **critical value** of f is the value of f at the critical point.
- The Belyi function corresponding to a dessin $\mathcal{D}$ is a **rational function** $f(x)$ of degree n if $\mathcal{D}$ may be embedded into the Riemann sphere $\hat{\mathbb{C}}$ in such a way that (i) the **black** vertices are the roots of $f(x) = 0$ with multiplicity equal to the degree of the corresponding (black) vertex, (ii) the **white** vertices are the roots of $f(x) = 1$ with multiplicity equal to the degree of the corresponding (white) vertex, (iii) the bicolored graph is the **preimage** of the segment $[0, 1]$, that is $\mathcal{D} = f^{-1}([0, 1])$, (iv) there exists **a single pole** of $f(x)$, i. e. a root of $f(x) = \infty$ **at each face**, the multiplicity of the pole equal to the degree of the face, and, finally, (v) besides 0, 1 and ∞, there are **no other critical values** of f.

Groth. 5: from dessins to incidence geometries

- In many cases one may establish a bijection between **notable point/line incidence geometries** $\mathcal{G}^i_{\mathcal{D}}$ to a dessin $\mathcal{D}$, $i = 1, \cdots, m$ with m being the number of non-isomorphic subgroups S of P that **stabilize a pair of its elements**.
- We ask that **every pair** of points on a line **shares the same stabilizer** in P. Thus given S a subgroup of P which stabilizes a pair of points, we define the point-line relation on $\mathcal{G}_{\mathcal{D}}$ such that two points will be adjacent if their stabilizer is isomorphic to S.
- Presumably, this action of the group P of a dessin $\mathcal{D}$ on the associated geometry $G_{\mathcal{D}}$ is intricately linked with the properties of the absolute Galois group $\Gamma = \mathrm{Gal}(\bar{\mathbb{Q}}/\mathbb{Q})$, which is the group of automorphisms of the field $\bar{\mathbb{Q}}$ of algebraic numbers.
- The built geometries may be seen as (non-local/contextual) **quantum geometries**: their coordinates are n-qubit observables.

Bell's theorem from the square geometry: 1

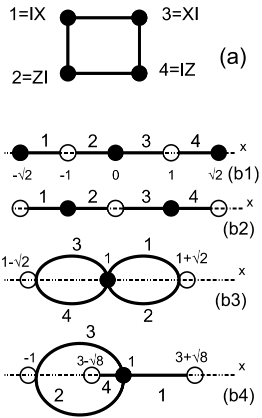

- A simple observable proof of Bell's theorem embodied in the geometry of a square (a) and four associated *dessins d'enfants*, (b_1) to (b_4).

Bell's theorem from the square geometry: 2

- **Dessin (b1)**: signature $s = (B, W, F, g) = (3, 2, 1, 0)$, group $P = \langle(2,3),(1,2)(3,4)\rangle$, cycle structure $[2^1 1^2, 2^2, 4^1]$ and Belyi function $f(x) = x^2(2 - x^2)$. The critical points are $x \in \{-1, 1, 0\}$ and the critical values are $\{1, 1, 0\}$. Preimage of the value 0 (solutions of $f(x) = 0$) corresponds to black vertices at $x \in \{-\sqrt{2}, \sqrt{2}, 0\}$. Preimage of the value 1 (solutions of $f(x) = 1$) corresponds to the white vertices at $x = \pm 1$.
- **Dessin (b2)**: $s = (2, 3, 1, 0)$, $P = \langle(1,2)(3,4),(2,3)\rangle$, cycles $[2^2, 2^1 1^2, 4^1]$ and Belyi function $f(x) = (x^2 - 1)^2$.
- **Dessin (b3)**: Belyi function $f(x) = \frac{(x-1)^4}{4x(x-2)}$. As $f'(x) = \frac{(x-1)^3(x^2-2x-1)}{2(x-2)^2x^2}$, its critical points lie at $x = 1$ (where $f(1) = 0$) and at $x = 1 \pm \sqrt{2}$ (where $f(1 \pm \sqrt{2}) = 1$).
- **Dessin (b4)**: Belyi function $f(x) = \frac{(x-1)^4}{16x^2}$.
- It is intriguing to see that all preimages in $\mathbb{P}_1$ live in the extension field $\mathbb{Q}(\sqrt{2}) \in \bar{\mathbb{Q}}$ of the rational field $\mathbb{Q}$.

The stellated octahedron

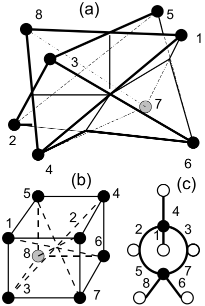

- The stellated octahedron (a), the completed cube (b) and their common stabilizing *dessin* (c). Belyi function

$$f(x) = K\frac{(x-1)^4(x-a)^4}{x^3}, \quad a = \frac{8\sqrt{10}-37}{27}, \quad K \approx -0.4082.$$

"Critical" white vertices $x \approx 0.0566 \pm 0.506i$, the other four white vertices at $x = -1.069$, $x = -0.162$ and $x = 1.634 \pm 0.6109i$.

Mermin square

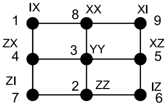

(a)

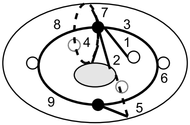

(b)

- A 3×3 grid with points labeled by two-qubit observables (*aka* a Mermin magic square) (a) and a stabilizing *dessin* drawn on a torus (b).

Mermin pentagram

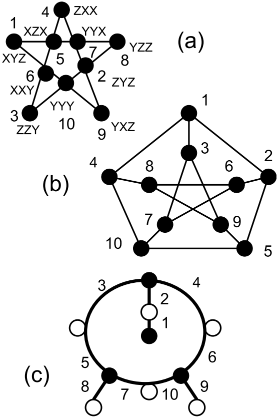

- The Mermin pentagram (a), the Petersen graph (b) and their generating *dessin* (c).

Desargues configuration

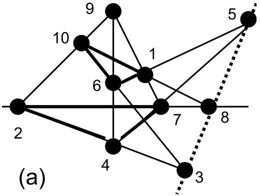

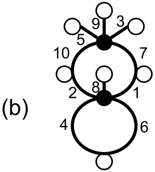

- The Desargues configuration (a) and its generating *dessin* (b).

Cremona-Richmund configuration and its two-qubit coordinates

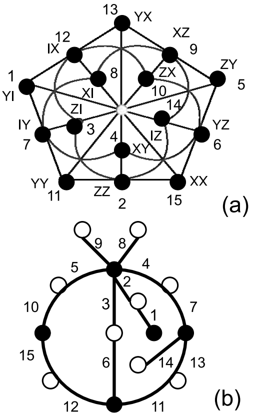

- The Cremona-Richmond 15_3-configuration (a) with its points labeled by the elements of the two-qubit Pauli group and its stabilizing *dessin* (b).

Three-qubit coordinatization of the generalized hexagon $GH(2,2)$ [and a unique extension of a 'magic' WA configuration to an hyperplane of type $V_{22}(37;0,12,,15,10)$].[14]

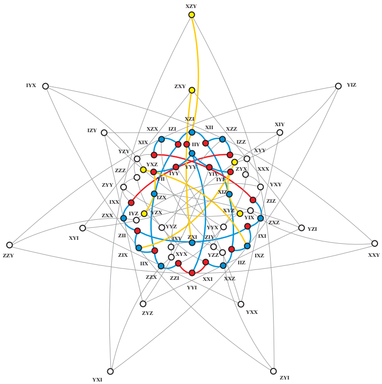

[14] M. Saniga, M. Planat, P. Pracna and P. Lévay, 'Magic' Configurations of Three-Qubit Observables and Geometric Hyperplanes of the Smallest Split Cayley Hexagon, SIGMA 8 (2012), 083, 9 pages.

We look at the **conjugacy classes of index** 63 of the group

$$\Gamma = \left\langle \rho_0, \rho_1, \rho_2 | \rho_1^2 = \rho_2^4 = (\rho_2\rho_1)^7 = (\rho_2^{-1} * \rho_1^{-1} * \rho_2 * \rho_1) = \rho_0\rho_1\rho_2 = 1 \right\rangle$$

and select the two corresponding to a dessin of permutation group P isomorphic to $S_3 \wr S_3$. There are just **two dessins** satisfying this requirement. The **first dessin** is of genus 0, signature $(35, 21, 9, 0)$ and cycle structure $[4^{28}1^7, 4^{12}2^6 1^3, 7^9]$. One finds three non isomorphic subgroups stabilizing a pair of elements of P, there are isomorphic to $\mathbb{Z}_6$ or D_4, or $\mathbb{Z}_2^3 \rtimes \mathbb{Z}_2^2$. The last one stabilizes the geometry of **the split Cayley hexagon** $GH(2,2)$ shown in Fig. 5. **The second dessin** is of genus 1, signature $(36, 18, 9, 1)$ and cycle structure $[2^{27}1^9, 4^{14}2^3 1^1, 7^9]$. Again one finds three non isomorphic subgroups stabilizing a pair of elements of P, there are isomorphic to $\mathbb{Z}_6$ or D_4, or is the extraspecial group E_{32}^+. The latter group stabilizes **the dual of** $GH(2,2)$.

Recovering the generalized hexagon $GH(2,2)$: index 63 in C_2^+

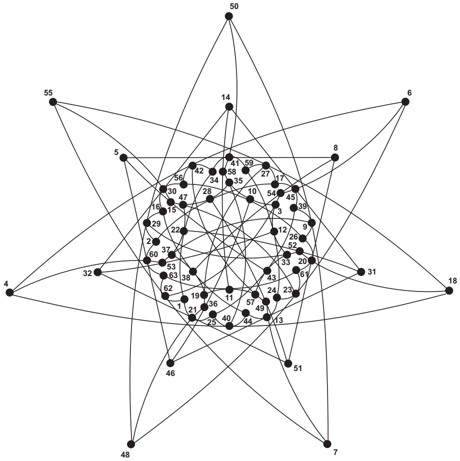

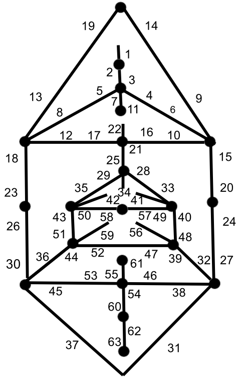

- A *dessin* (right) for the generalized hexagon $GH(2,2)$ (left).

Recovering a generalized hexagon: index 63 in C_2^+

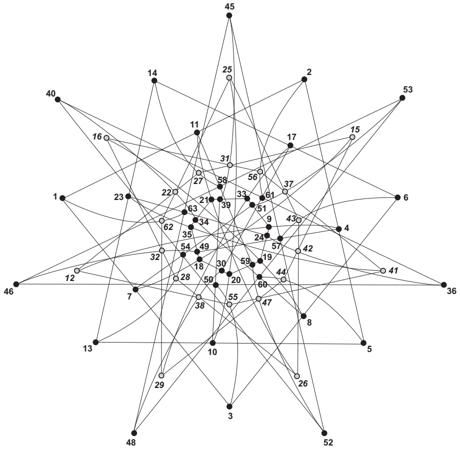

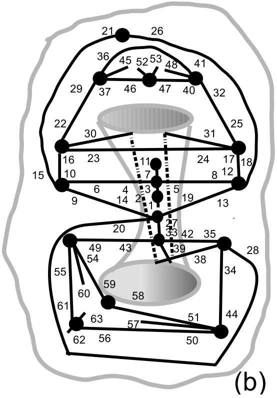

- A *dessin* (right) for the dual of the generalized hexagon $GH(2,2)$ (left).

Generalized polygons and their hyperplanes: relating the (non-partitioning) parts and the whole

- A **generalized polygon** (or generalized n-gon) is an **incidence structure** between a discrete set of points and lines whose incidence graph has diameter n and girth $2n$. A generalized n-gon cannot contain i-gons for $2 \leq i < n$ but can contain ordinary n-gons. A **generalized polygon of order** (s, t) is such that every line contains $s + 1$ points and every point lies on $t + 1$ lines. A **projective plane** of order n is a generalized 3-gon. The generalized 4-gons are the **generalized quadrangles**. Generalized 5-gons, 6-gons, etc are also called **generalized** pentagons, **hexagons**, etc.
- A **geometric hyperplane** of a generalized polygon is a proper subspace meeting each line at a unique point or containing the whole line. For a polygon of order $(2, t)$ such hyperplanes of a n-gon satisfy (and are usefully built from) the following set theoretical equation between hyperplanes H, H' and H"

$$H" = H \oplus H' = \overline{H \Delta H'}, \text{ for any } H \text{ and } H', \tag{9}$$

where Δ means the **symmetric difference** and the overline symbol means the **complement**.

The generalized hexagon $GH(2,1)$

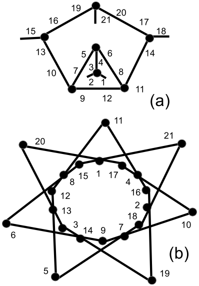

- Dessin for $GH(2,1)$: One selects, in the 13740 conjugacy classes of index 21 of the modular group $\Gamma = \left\langle \rho_0, \rho_1, \rho_2 | \rho_1^2 = \rho_2^3 = \rho_0\rho_1\rho_2 = 1 \right\rangle$, the unique one whose dessin that has a permutation group P isomorphic to $PSL(2,7)$. One then finds three non isomorphic subgroups of P stabilizing a pair of elements of P, there are isomorphic to the groups $\mathbb{Z}_1$, $\mathbb{Z}_2$ and $\mathbb{Z}_2^2$, respectively. The latter group induces the geometry of the hexagon $GH(2,1)$. The signature is $(7,13,3,0)$ with cycle structure $[3^7, 2^8 1^5, 7^3]$.

Hyperplanes of the generalized hexagon $GH(2,1)$

The **hyperplane structure** comprises **six types** that can easily be derived **from a single type**, the perp-set one H_4, by using the hyperplane sum relation (9). The perp-set type of hyperplane contains all vertices of the collinearity graph at distance ≤ 2 from a selected vertex. Taking **all sums** $H_4 \oplus H_4$ over the distinct hyperplanes, one gets all hyperplanes of type H_{2b} (42 copies) and H_3 (84 copies). Then, all sums $H_{2a} \oplus H_4$ lead to the 24 hyperplanes of type H_1 and the 56 ones of type H_{2a}; further sums of type $H_1 \oplus H_2$ create the collection of hyperplanes of type H_5. There are 2^8 hyperplanes.

Class	Pts	Lns	n_0	n_1	n_2	Cps	Remark
H1	7	0	7	0	0	24	ovoid
H2a	9	2	3	6	0	56	
H2b	9	2	4	4	1	42	
H3	11	4	2	6	3	84	
H4	13	6	0	8	5	21	perp-set
H5	15	8	0	6	9	28	

The 14 classes of the 2^{16} hyperplanes of the dual of $GH(2,2)$ (that covers $GH(2,1)$)

Class	Pts	Lns	DPts	Cps	StGr	FJ Type
I	23	3	1	252	$Q_8 : S_3$	$\mathcal{W}_3(23;16,6,0,1)$
II	27	9	1	2016	S_3	$\mathcal{W}_{10}(27;8,12,6,1)$
	27	9	0	2016	S_3	$\mathcal{W}_{12}(27;6,15,6,0)$
III	31	15	1+6	63	$X_{32}^+ : S_3$	$\mathcal{W}_1(31;0,24,0,7)$
	31	15	3(1+2)	378	$(2\times 4)\cdot 2^2$	$\mathcal{W}_6(31;0,20,8,3)$
	31	15	1+2+3	1008	D_{12}	$\mathcal{W}_8(31;4,15,6,6)$
	31	15	2	3024	2^2	$\mathcal{W}_{13}(31;4,11,14,2)$
	31	15	1+2	3024	2^2	$\mathcal{W}_{14}(31;4,12,12,3)$
IV	35	21	7	864	D_{14}	$\mathcal{W}_7(35;0,14,14,7)$
	35	21	1+2+3	2016	S_3	$\mathcal{W}_{11}(35;2,9,18,6)$
V	39	27	3+6	252	$2\times S_4$	$\mathcal{W}_4(39;0,6,24,9)$
	39	27	3+9	336	$S_3\times S_3$	$\mathcal{W}_5(39;0,9,18,12)$
	39	27	3+3+6	1008	D_{12}	$\mathcal{W}_9(39;0,9,18,12)$
VI	47	39	1+6+16	126	$(4\circ Q_8) : S_3$	$\mathcal{W}_2(47;0,0,24,23)$

The generalized octagon $GO(2,1)$

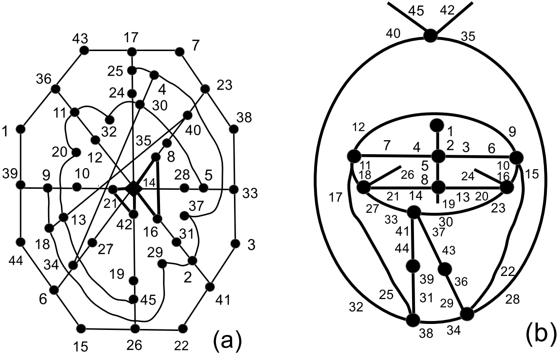

The octagon $GO(2,1)$: 45 points and 30 lines. One selects the group of order 360 in $\Gamma = \left\langle \rho_0, \rho_1, \rho_2 | \rho_1^2 = \rho_2^4 = (\rho_1 \rho_2^{-1})^5 = 1 \right\rangle$. (B. De Bruyn, Preprint 2011).

The 2^{16} hyperplanes of the generalized octagon $GO(2,1)$ in 34 classes

Class	Pts	Lns	Cps	FJ Type
I	15	0	288	$\mathcal{X}_1(15;15,0,0)$
II	17	2	2880	$\mathcal{X}_2(17;11,6,0)$
	17	2	1080	$\mathcal{X}_3(17;12,4,1)$
III	19	4	1440	$\mathcal{X}_4(19;7,12,0)$
	19	4	4320	$\mathcal{X}_5(19;9,8,2)$
	19	4	4320	$\mathcal{X}_6(19;8,10,1)$
	19	4	1440	$\mathcal{X}_7(19;10,6,3)$
IV	21	6	2160	$\mathcal{X}_8(21;5,14,2)$
	21	6	360	$\mathcal{X}_9(21;4,16,1)$
	21	6	2340	$\mathcal{X}_{10}(21;8,8,5)$
	21	6	4320	$\mathcal{X}_{11}(21:7,10,4)$
	21	6	6360	$\mathcal{X}_{12}(21;6,12,3)$
V	23	8	3960	$\mathcal{X}_{13}(23;6,10,7)$
	23	8	5040	$\mathcal{X}_{14}(23;5,12,6)$
	23	8	2880	$\mathcal{X}_{15}(23;3,16,4)$
	23	8	2880	$\mathcal{X}_{16}(23:4,14,5)$
VI	25	10	36	$\mathcal{X}_{17}(25;0,20,5)$
	25	10	5040	$\mathcal{X}_{18}(25;4,12,9)$
	25	10	720	$\mathcal{X}_{19}(25;1,18,6)$
	25	10	1584	$\mathcal{X}_{20}(25;5,10,10)$
	25	10	1440	$\mathcal{X}_{21}(25;3,14,8)$
	25	10	1440	$\mathcal{X}_{22}(25;2,16,7)$
VII	27	12	360	$\mathcal{X}_{23}(27;4,10,13)$
	27	12	2880	$\mathcal{X}_{24}(27;2,14,11)$
	27	12	1440	$\mathcal{X}_{25}(27;3,12,12)$
	27	12	240	$\mathcal{X}_{26}(27;0,18,9)$
VIII	29	14	720	$\mathcal{X}_{27}(29;1,14,14)$
	29	14	225	$\mathcal{X}_{28}(29;0,16,13)$

Information stored in hyperplanes of finite geometries induced by dessins d'enfants

Geometry	Pts	Lns	bits	Cls	Remark
5-cell	5	10	**1**	1	
octahedron	6	8	**2**	1	
Fano plane	7	7	**3**	1	
Pappus	9	9	2	1	
GQ(2,1)	9	6	4	2	alias the (3×3)- grid
$\bar{K}(3)^3$	9	27	6	3	gen hyp
Desargues	10	10	**4**	2	
GQ(2,2)	15	15	**5**	3	alias Cremona-Richmund
GH(2,1) $\equiv S_{1,1}$	21	14	**8**	6	
GQ(2,4)	27	45	6	2	
Pappus 3-fold cover	27	27	8	9	
$S_{1,1,1}$ (*)	27	27	8	5	alias the $(3 \times 3 \times 3)$-grid
$\tilde{GQ}(2,2)$	45	45	**11**	15	
GO(2,1)	45	30	**16**	34	
GH(2,2)	63	63	14	25	a 'split Cayley hexagon'
GH(2,2) dual	63	63	14	14	
$S_{1,1,1,1}$(*)	81	108	16	29	alias the $(3 \times 3 \times 3 \times 3)$-grid